

Article

# Compatibility between C<sub>6</sub>F<sub>12</sub>O–N<sub>2</sub> Gas Mixture and Metal Used in Medium-Voltage Switchgears

Ran Zhuo <sup>1,2</sup>, Qi Chen <sup>3,\*</sup>, Dibo Wang <sup>1,2</sup>, Mingli Fu <sup>1,2</sup>, Ju Tang <sup>3</sup>, Juntai Hu <sup>4</sup> and Yanlei Jiang <sup>4</sup>

<sup>1</sup> Electric Power Research Institute, China Southern Power Grid, Guangzhou 510623, China; zhuoran@csg.cn (R.Z.); wangdb@csg.cn (D.W.); fuml@csg.cn (M.F.)

<sup>2</sup> State Key Laboratory of HVDC, Electric Power Research Institute, CSG, Guangzhou 510663, China

<sup>3</sup> School of Electrical Engineering and Automation, Wuhan University, Wuhan 430072, China; whtangju@whu.edu.cn

<sup>4</sup> Pingdingshan Power Supply Company, State Grid Corporation of China, Pingdingshan 467001, China; jy1020406@sina.com (J.H.); jy12500@sina.com (Y.J.)

\* Correspondence: chenqimails@163.com; Tel.: +86-1582-7459-572

Received: 4 November 2019; Accepted: 1 December 2019; Published: 6 December 2019



**Abstract:** C<sub>6</sub>F<sub>12</sub>O has been introduced as the potential alternative gas to SF<sub>6</sub> because of its excellent insulation properties and great eco-friendly performance. Considering that C<sub>6</sub>F<sub>12</sub>O may react with the internal materials of switchgears in practical applications, its compatibility with metal materials must be tested to evaluate its long-term application possibilities. In this work, the compatibility of C<sub>6</sub>F<sub>12</sub>O–N<sub>2</sub> gas mixtures with aluminum and copper was tested at different temperatures by setting up a heat-aging reaction platform between the gas and each metal. The metal surface morphology and gas composition before and after the reaction were compared and analyzed. The results show that the surface color of the copper sheet changed considerably, and the corrosion degree of the surface deepened with the increase of temperature. The decomposition of C<sub>6</sub>F<sub>12</sub>O was also promoted. In contrast, aluminum did not react severely with the gas mixture. The compatibility of the gas mixture with aluminum was generally better than that of copper.

**Keywords:** SF<sub>6</sub> alternative gas; C<sub>6</sub>F<sub>12</sub>O–N<sub>2</sub> gas mixture; material compatibility; copper; aluminum

## 1. Introduction

SF<sub>6</sub> has been widely used in the power industry, especially in high-voltage (HV) and medium-voltage (MV) gas-insulated switchgears (GIS), since the early 1980s due to its excellent technical performance and small footprint [1,2]. Approximately 80% of the global production of SF<sub>6</sub> is used in HV and MV gas-insulated equipment [3,4]. However, SF<sub>6</sub> has a high global warming potential (GWP) of 23,500 and a long atmospheric lifetime of 3200 years [5,6]. These characteristics indicate that the unrestricted emission of SF<sub>6</sub> would cause great harm to the atmospheric environment. Actually, the atmospheric content of SF<sub>6</sub> increases rapidly. The global annual mean concentration of SF<sub>6</sub> in 2011 was 7.29 ppt, which is 1.65 ppt higher than the value in 2005 [7]. Thus, the Kyoto Protocol in 1997 and the Paris Agreement in 2015 were proposed to implement measures for controlling SF<sub>6</sub> growth [8,9], and several countries have begun to take action. For example, Slovenia and Spain have levied SF<sub>6</sub> emission taxes [10]. Therefore, the use of SF<sub>6</sub> should be urgently reduced or limited, and an environmental-friendly gas must be identified to replace SF<sub>6</sub>.

The gases currently used in switchgears mainly include CO<sub>2</sub>, N<sub>2</sub>, dry air, SF<sub>6</sub>, and their gas mixtures. However, due to the limited insulation strength of traditional gases (up to approximately 30%–40% of that of SF<sub>6</sub>) [11], the filling pressure or dimension must be increased when these gases are

used as the insulating or arc extinguishing medium in the equipment. This condition entails security risks and increased equipment cost [12].

In addition to the traditional gases mentioned above, potential alternatives to SF<sub>6</sub> that have been considered in recent years include perfluorocarbons (PFCs), trifluoriodomethane (CF<sub>3</sub>I), HFO-1234zeE, fluoronitrile (C<sub>4</sub>F<sub>7</sub>N), and fluoroketones (C5-PFK and C6-PFK). The GWP of PFCs is high (e.g., c-C<sub>4</sub>F<sub>8</sub> and C<sub>2</sub>F<sub>6</sub> have GWPs of 8700 and 12,200, respectively); thus, there is no significant reduction in GWP [13–15]. CF<sub>3</sub>I is classified as a type 3 mutagen and presents disadvantages such as iodine I<sub>2</sub> (acute toxicity) precipitation after repeated discharges. Therefore, it is not conducive for long-term safe equipment operation [16,17]. HFO-1234zeE will precipitate carbon deposits on the solid after a flashover and have a risk of flammability [3,18]. C<sub>4</sub>F<sub>7</sub>N demonstrates excellent insulation performance, but its toxicity is relatively high, and the risks of large-scale engineering application still require further study [19–21]. The application prospect of fluoroketones in electrical equipment has been widely optimistic in the past few years, and related research has mainly focused on C5-PFK and C6-PFK gas mixtures. Table 1 shows a comparison of several of the main characteristics of C5-PFK, C6-PFK, and SF<sub>6</sub> [22–25]. It can be seen that C6-PFK is less toxic than C5-PFK.

**Table 1.** Comparison of C5-PFK, C6-PFK, and SF<sub>6</sub> GWP: global warming potential.

Name	C5-PFK	C6-PFK	SF <sub>6</sub>
Chemical formula	C <sub>5</sub> F <sub>10</sub> O	C <sub>6</sub> F <sub>12</sub> O	SF <sub>6</sub>
GWP	<1	<1	23500
Atmospheric lifetime (years)	0.04	0.019	3200
Ozone depletion potential	0	0	0
Boiling point at 0.1 MPa (°C)	24	49.2	−64
Relative dielectric strength to SF <sub>6</sub>	2	2.5	1
Flammability	non-flammable	non-flammable	non-flammable
Toxicity (LC50, ppm <sub>v</sub> )	>20000	>100000	>100000

Currently, C<sub>6</sub>F<sub>12</sub>O is only used as a fire-extinguishing agent and covering gas for magnesium treatment as well as two-phase immersion cooling systems, which is safe to use and relatively low in cost [26]. Furthermore, research on C<sub>6</sub>F<sub>12</sub>O as a gas-insulating medium has just started [27–30]. However, due to its high boiling point, C<sub>6</sub>F<sub>12</sub>O cannot be used as an insulating medium alone; that is, it must be mixed with a buffer gas, such as N<sub>2</sub> or CO<sub>2</sub>. Moreover, since the dielectric strength of pure C6-PFK can reach about 2.5 times that of SF<sub>6</sub>, a gas mixture with a small percentage of C6-PFK can also achieve a relatively high insulation strength. Relevant results demonstrate that C<sub>6</sub>F<sub>12</sub>O gas mixtures have the potential to be used in MV switchgears, such as cubicle gas-insulated switchgears (C-GIS) [31].

In addition, in-depth studies of the long-term compatibility between gas-insulating medium and materials must be conducted. Given that C<sub>6</sub>F<sub>12</sub>O gas is not as inert as SF<sub>6</sub>, chemical reactions might exist between the gas components and materials, resulting in changes in the properties of materials and jeopardizing the normal operation of gas-insulated equipment. Thus, material compatibility must be tested before engineering application to avoid any negative effect of the interaction between the materials and the C<sub>6</sub>F<sub>12</sub>O–N<sub>2</sub> gas mixture.

In this study, considering that the advantage of CO<sub>2</sub> is its arc-extinguishing ability and that the C<sub>6</sub>F<sub>12</sub>O gas mixtures are mainly used in non-arcing applications, the N<sub>2</sub> with an extremely low boiling point was chosen as the carrier gas to reduce the liquefaction temperature of the gas mixture. The compatibility of C<sub>6</sub>F<sub>12</sub>O–N<sub>2</sub> gas mixtures with copper and aluminum, which are normally used in medium-voltage switchgears (e.g., C-GIS) as conductors, was studied by aging tests. The surface morphology of the metals and the composition of the gas mixtures after thermal aging were determined and analyzed via scanning electron microscopy (SEM) and gas chromatography-mass spectrometry (GCMS). The interaction mechanism between the gas mixture and metallic surface was also discussed. Relevant results could provide guidance for the engineering application of C<sub>6</sub>F<sub>12</sub>O–N<sub>2</sub> gas mixtures.

## 2. Experimental Device and Methods

The experimental device, experimental methods, and analytical methods used in this paper are described in detail as follows.

### 2.1. Experimental Device

The schematic of the compatibility test device is shown in Figure 1.

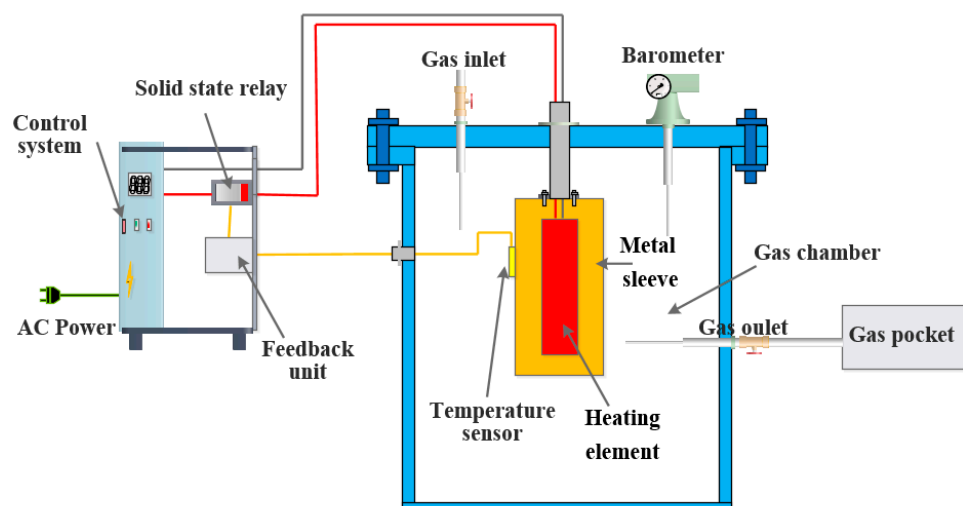


Figure 1. Schematic of the compatibility test device.

The test device mainly consisted of a gas chamber, heating device, temperature feedback unit, and control system. The heating device was composed of a heating element and a metal sleeve. The metal sleeve was used to expand the contact area with the  $C_6F_{12}O-N_2$  gas mixture, and the outer surface of the metal sleeve served as the reaction interface with the gas mixture. The metal sleeve and heating element were kept in close contact to achieve even heat conduction. Moreover, two  $100\text{ mm} \times 5\text{ mm} \times 0.2\text{ mm}$  metal sheets were bundled on the metal sleeve to participate in the thermal aging test. The metal sleeves and sheets were composed of copper or aluminum according to the experimental requirements. The feedback unit detected the surface temperature of the metal sleeve through a temperature sensor (K-type thermocouple) mounted on the metal sleeve surface. The temperature control system adjusted the output power of the heating element to ensure that the surface temperature of the metal sleeve remained at the set value during the tests. The main body and the upper cover of the gas chamber are welded and machined with 304 stainless steel (due to its great corrosion resistance performance), as well as polished inside and outside. The chamber can withstand a pressure of 0.7 MPa, and its volume is about 2 L.

### 2.2. Experimental and Analytical Methods

Prior to the experiment, the gas chamber, metal sleeve, and metal sheet were carefully cleaned using absolute alcohol, and the metal sheet was fixed to the metal sleeve. The gas chamber was vacuumed and then filled with  $N_2$  three times to dispel the gas impurity. Finally, the gas mixture was charged into the gas chamber. The volume fraction was determined by a partial pressure ratio based on the Dalton partial pressure law. When inflating, the  $C_6F_{12}O$  was charged first, followed by the buffer gas. The  $N_2$  is supplied by Wuhan Newred Special Gas Co., Ltd. with a purity of 99.999%. The  $C_6F_{12}O$  gas is supplied by Zhengzhou Alfachem Co., Ltd. with a purity of 99%.

Given the working pressure and liquefaction temperature requirements ( $-5\text{ }^\circ\text{C}$ ) of MV switchgears [32], the total gas pressure and content of  $C_6F_{12}O$  in the experiment were fixed to 0.2 MPa and 5%, respectively. The breakdown voltage of 5%  $C_6F_{12}O-95\%$   $N_2$  gas mixture at 0.2 MPa is about

1.05 times that of 10% SF<sub>6</sub>–90% N<sub>2</sub> [29]. Considering the temperature rise effect of the current-carrying metal inside the equipment under the rated working condition and the local overheating faults caused by the poor contact of the contacts, the experimental temperature was set to 150 °C, 200 °C, and 250 °C. Each set of experiments was heated for 8 h.

The gas in the chamber was collected for GC-MS analysis after each group of tests. When the gas is scanned by GC-MS, the range of the mass-to-charge ratios (*m/z*) is set to 45–350 to remove the damage of the detector by the oversaturation of N<sub>2</sub> and the interference of H<sub>2</sub>O and CO<sub>2</sub> in the air. The surface morphology of the metal sheets before and after thermal aging was observed and recorded with optical and scanning electron microscopes.

### 3. Results of Compatibility between C<sub>6</sub>F<sub>12</sub>O–N<sub>2</sub> Gas Mixture and Cooper

In order to comprehensively analyze the compatibility between the C<sub>6</sub>F<sub>12</sub>O–N<sub>2</sub> gas mixture and copper, the surface morphology of the copper sheets and the gas composition before and after the reaction were analyzed by optical microscope, SEM.

#### 3.1. Surface Morphology

Figure 2 shows surface morphology photos of the copper sheet before and after thermal aging for 8 h.

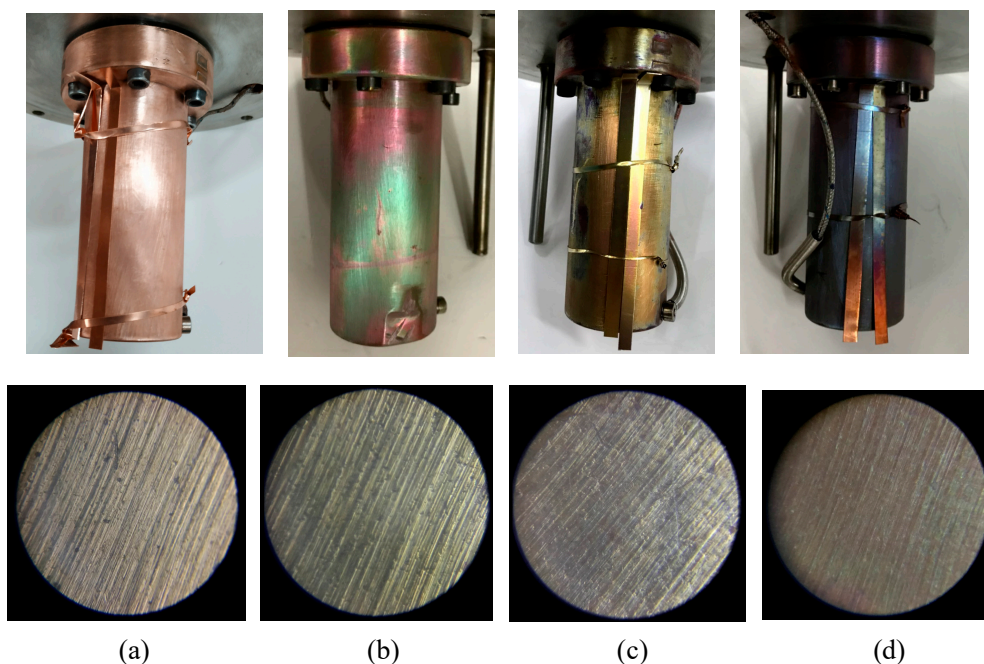


**Figure 2.** Surface morphology photos of the copper sheet before and after thermal aging. (a) Before the test; (b) 150 °C; (c) 200 °C; (d) 250 °C.

It can be found that several areas of the copper sheet changed to red and green after an 8 h test at 150 °C. The surface color of the copper sheet deepened as the temperature increased. The copper surface turned bright orange at 200 °C, and most of the area turned purple–red at 250 °C, indicating that a significant chemical reaction occurred between the copper and the gas mixture. Meanwhile, the optical microscope showed that the grain structure on the copper sheet gradually became less clear as the temperature increased. These phenomena indicate that the material compatibility between copper and the C<sub>6</sub>F<sub>12</sub>O–N<sub>2</sub> gas mixture was not very good, and the reactions resulted in a significant surface change.

In order to facilitate comparative analysis with SF<sub>6</sub>, the copper sheets exposed to a 220 °C SF<sub>6</sub> environment for 8 h were also tested, and it was found that there is no significant change in the color

of the copper surface. The relevant results confirm that the compatibility between copper and  $\text{SF}_6$  is superior to that between copper and the  $\text{C}_6\text{F}_{12}\text{O}-\text{N}_2$  gas mixture.

Actually, when the  $\text{C}_6\text{F}_{12}\text{O}$  gas mixture is in contact with the heated copper surface, the thermal motion of  $\text{C}_6\text{F}_{12}\text{O}$  molecules and Cu atoms is intensified, which causes the intensification of the chemical bond vibration inside the molecule and the deterioration of the structure stability, eventually leading to a chemical reaction between the gas molecule and the heated copper surface. As the temperature increases, the reaction rate is further accelerated, causing the decomposition of gas molecules and severe corrosion of the copper surface.

### 3.2. SEM Analysis

SEM was used to observe the surface morphology and further analyze the microscopic morphology of the copper sheet. The observation results are shown in Figure 3. The surface shape of the copper sheet before the reaction was clear, and the structure was flat and compact. Fewer corrosion spots were observed at 150 °C, and the texture was not damaged. As the temperature increased further, the surface of the copper sheet became uneven, indicating that serious corrosion occurs at this stage.

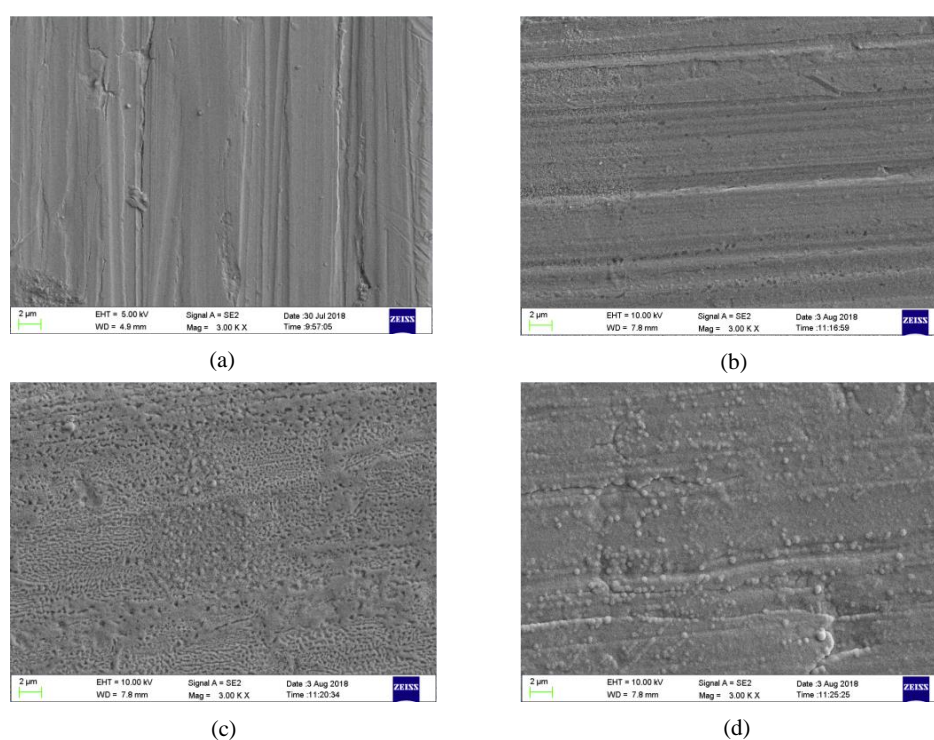


**Figure 3.** Surface morphology photos of the copper sheet before and after thermal aging at 3000 times magnification. (a) Before the test; (b) 150 °C; (c) 200 °C; and (d) 250 °C.

### 3.3. GC-MS Analysis

Qualitative analysis of the gas mixture after the aging test was performed in accordance with the National Institute of Standards and Technology's (NIST 14.0) standard chromatographic database [33]. Given that the gas composition after the experiment was unknown, the gas could only be qualitatively analyzed using the SCAN mode. Figure 4 shows the gas chromatogram of the  $\text{C}_6\text{F}_{12}\text{O}-\text{N}_2$  gas mixtures before and after the experiment.

It can be seen from Figure 4 that the  $\text{C}_6\text{F}_{12}\text{O}-\text{N}_2$  gas mixture decomposed at 150 °C, and the main decomposition products included  $\text{C}_4\text{F}_8\text{O}$ ,  $\text{C}_3\text{F}_6$ , and  $\text{C}_2\text{F}_5\text{H}$ . With the increase in temperature, the peak areas of  $\text{C}_3\text{F}_6$  and  $\text{C}_2\text{F}_5\text{H}$  increased considerably. This result indicates that the macromolecular product decomposed further with the increase in temperature. The production of  $\text{C}_2\text{F}_5\text{H}$  may be related to trace moisture.

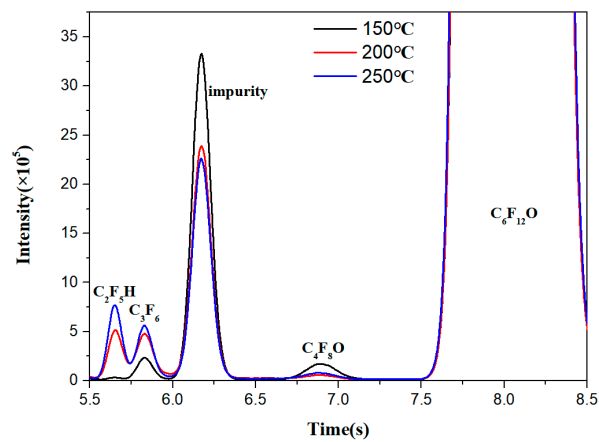


**Figure 4.** Gas chromatography of the C<sub>6</sub>F<sub>12</sub>O–N<sub>2</sub> gas mixtures.

According to the surface morphology change of the copper sheet and the composition change of the C<sub>6</sub>F<sub>12</sub>O–N<sub>2</sub> gas mixtures before and after the reaction, the C<sub>6</sub>F<sub>12</sub>O–N<sub>2</sub> gas mixtures interacted with the copper sheet at 150 °C and above, and the surface structure of the copper sheet exhibited certain corrosion. The gas mixtures decomposed to produce decomposition products, such as C<sub>2</sub>F<sub>5</sub>H and C<sub>3</sub>F<sub>6</sub>. The compatibility of the C<sub>6</sub>F<sub>12</sub>O–N<sub>2</sub> gas mixtures with copper was not very good, and the mutual reaction between them may pose a potential threat to gas-insulated equipment.

#### 4. Results of Compatibility between C<sub>6</sub>F<sub>12</sub>O–N<sub>2</sub> Gas Mixtures and Aluminum

Similarly, the results of analysis by optical microscope, SEM, and GC-MS before and after the reaction are as follows.

##### 4.1. Surface Morphology

Figure 5 shows surface morphology photos of the aluminum sheet before and after the high-temperature 8 h aging test.

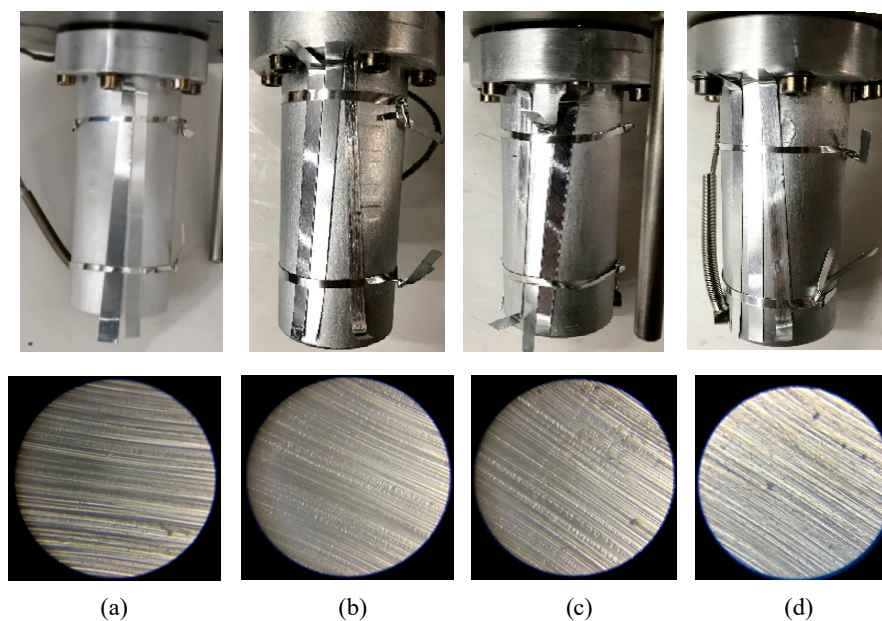


**Figure 5.** Surface morphology photos of the aluminum sheet before and after the high-temperature 8 h aging test. (a) Before the test; (b) 150 °C; (c) 200 °C; and (d) 250 °C.

After the high-temperature reaction of the aluminum sheet and  $C_6F_{12}O-N_2$  gas mixture, the surface color of the aluminum did not change considerably. The aluminum surface stayed white and silver, and the gloss was bright. The main reason for this phenomenon is that aluminum is more active and easily oxidized in air to form a dense  $Al_2O_3$  protective film, which is extremely resistant to corrosion and therefore forms an effective protection of the internal aluminum.

The results of optical microscopy show that the surface grain structure of the aluminum sheet was maintained with the increasing temperature, and no corrosion changes occurred. These phenomena indicate that the material compatibility between aluminum and the gas mixtures was great, and the reaction between the gas mixtures and aluminum sheet did not change the surface of the sheet.

#### 4.2. SEM Analysis

Figure 6 shows the SEM of the aluminum sheet before and after tests. The surface morphology of the aluminum was flat and tight, and no change was observed at all temperature conditions. No corrosion spots were observed.

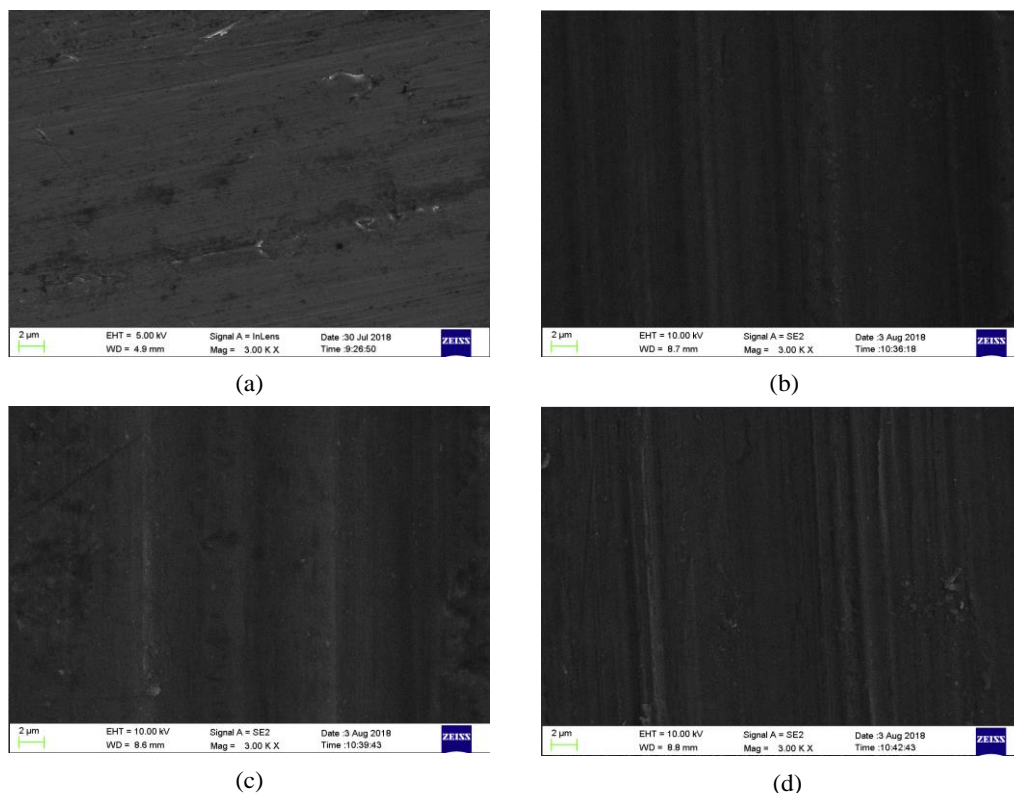


**Figure 6.** Surface morphology photos of the aluminum sheet before and after thermal aging at 3000 times magnification. (a) before the test; (b) 150 °C; (c) 200 °C; and (d) 250 °C.

#### 4.3. GC-MS Analysis

Figure 7 shows the gas chromatogram of the  $C_6F_{12}O-N_2$  gas mixtures after heat aging with aluminum for 8 h at different temperatures.

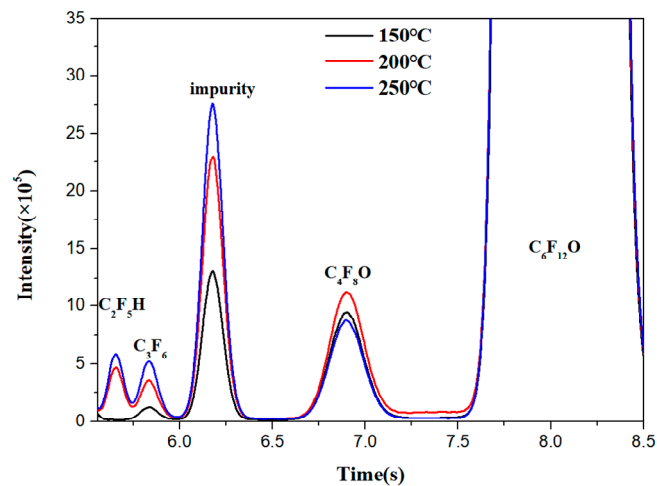


**Figure 7.** Gas chromatography of the  $C_6F_{12}O-N_2$  gas mixtures after thermal aging.

The chromatogram results show that the decomposition components of the  $C_6F_{12}O-N_2$  gas mixture that interacted with aluminum were similar to those of copper.  $C_2F_5H$ ,  $C_3F_6$ , and  $C_4F_8O$  were detected after the test. These results, together with the characterization results in Section 3.2, indicate that the surface structure of the aluminum sheet was not destroyed, so the appearance of this decomposition product is presumed to be a slight decomposition of  $C_6F_{12}O$  gas after heating.

Overall, the  $C_6F_{12}O-N_2$  gas mixture could interact with copper and aluminum at temperatures higher than  $150\text{ }^\circ\text{C}$ . The corrosion degree of the copper sheet was more serious than that of aluminum. The compatibility of the  $C_6F_{12}O-N_2$  gas mixture with aluminum is better than that of copper.

Thus, it is necessary to consider the reaction of the  $C_6F_{12}O-N_2$  gas mixture with copper materials used inside gas-insulated switchgears for engineering application, which would lead to internal insulation failure of the electrical equipment and pose safety hazards during normal long-term operation of the equipment.

## 5. Discussion

In fact, the reason why the material compatibility of the  $C_6F_{12}O-N_2$  gas mixtures with aluminum was better than with copper may be attributed to the difference in the activity of these two metal surfaces.

As we know, aluminum is more active and easily oxidized in air to form a dense  $Al_2O_3$  protective film, which is extremely resistant to corrosion and therefore forms an effective protection of the internal aluminum. The existence of  $Al_2O_3$  could effectively inhibit the interaction between aluminum and  $C_6F_{12}O-N_2$  gas mixtures.

In contrast, the chemical reactivity of copper is quite strong. When a  $C_6F_{12}O$  gas molecule interacts with the copper surface, the interaction between the gas molecule and the metal surface occurs along with charge transfer process. The structure of the gas molecule will change and the weaker chemical bonds in the  $C_6F_{12}O$  molecule will dissociate to form some particles. Finally, the reaction between the particles could result in the formation of gaseous by-products.

The possible reactions between the metal surface and  $C_6F_{12}O$  can be summarized as shown in Figure 8.

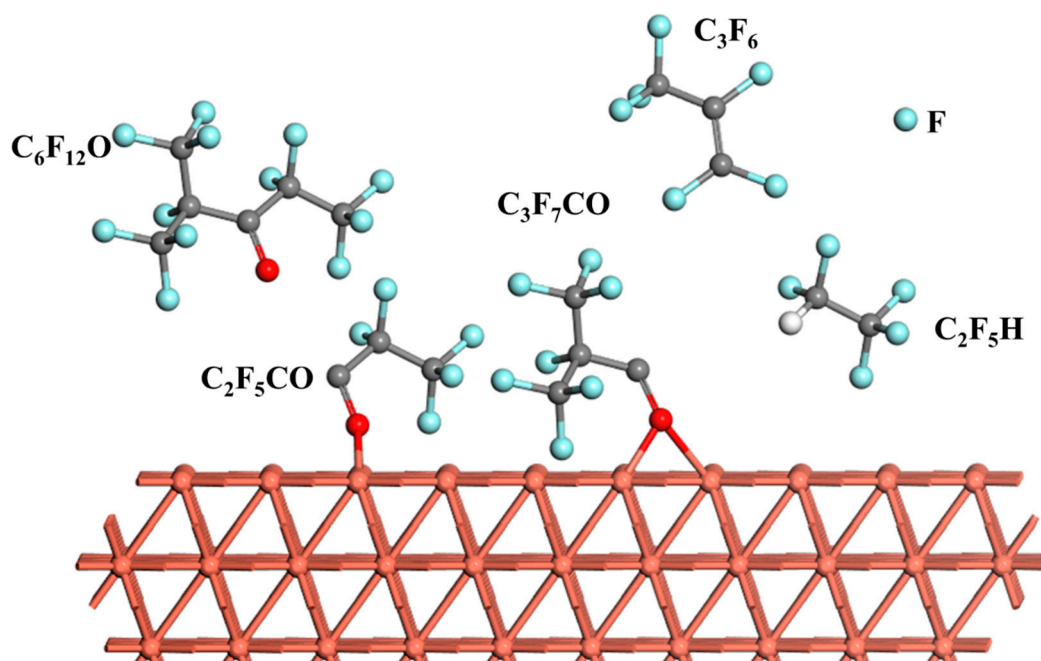


Figure 8. Interaction mechanism between  $C_6F_{12}O$  and copper.

## 6. Conclusions

In this work, the material compatibility of a potential  $SF_6$  substitute gas,  $C_6F_{12}O$ , with copper and aluminum was studied. Thermal aging test results at different temperatures were analyzed. The compatibility of the gas mixtures with copper and aluminum was evaluated by comparing the surface morphology of the metal materials and the composition of the  $C_6F_{12}O-N_2$  gas mixture before and after the reaction. The following relevant conclusions were obtained.

(1) The  $C_6F_{12}O-N_2$  gas mixture could react with hot copper higher than  $150\text{ }^\circ\text{C}$ . The surface structure of the copper sheet was corroded to some extent, the color change was evident, and the gas mixture decomposed to produce by-products including  $C_2F_5H$ ,  $C_3F_6$ , and  $C_4F_8O$ .

(2) The interaction of the  $C_6F_{12}O-N_2$  gas mixtures with aluminum under high-temperature conditions did not cause corrosion of aluminum surface, while the gas mixture also decomposed to produce  $C_3F_6$ ,  $C_2F_5H$ , and  $C_4F_8O$ .

(3) The compatibility of the  $C_6F_{12}O-N_2$  gas mixture with aluminum was better than that of copper. It is necessary to consider the reaction of the gas mixture with the copper used inside gas-insulated switchgears to avoid potential hazards during the normal long-term operation of the equipment.

**Author Contributions:** Q.C. conceived and designed the research, R.Z. performed the research and wrote this manuscript, while M.F., D.W., J.T., J.H. and Y.J. helped analyze the data.

**Funding:** This research was funded by China Southern Power Grid, grant number ZBKJXM20170090.

**Conflicts of Interest:** The authors declare no competing interests.

## References

- Hyrenbach, M.; Zache, S. Alternative insulation gas for medium-voltage switchgear. In Proceedings of the 2016 Petroleum and Chemical Industry Conference Europe (PCIC EUROPE), Berlin, Germany, 14 June–16 July 2016.
- Li, Y.; Zhang, X.; Zhang, J.; Tang, J.; Xie, C.; Shao, X.; Wang, Z.; Chen, D.; Xiao, S. Study on the thermal decomposition characteristics of  $C_4F_7N-CO_2$  mixture as eco-friendly gas insulating medium. *High. Volt.* **2019**. [[CrossRef](#)]

3. Beroual, A.; Haddad, A. Recent advances in the quest for a new insulation gas with a low impact on the environment to replace sulfur hexafluoride (SF<sub>6</sub>) gas in high-voltage power network applications. *Energies* **2017**, *10*, 1216. [[CrossRef](#)]
4. Li, Y.; Zhang, X.; Xiao, S.; Chen, Q.; Tang, J.; Chen, D.; Wang, D. Decomposition properties of C<sub>4</sub>F<sub>7</sub>N/N<sub>2</sub> gas mixture: An environmentally friendly gas to replace SF<sub>6</sub>. *Ind. Eng. Chem. Res.* **2018**, *57*, 5173–5182. [[CrossRef](#)]
5. Zhang, X.; Xiao, H.; Tang, J.; Cui, Z.; Zhang, Y. Recent advances in decomposition of the most potent greenhouse gas SF<sub>6</sub>. *Crit. Rev. Environ. Sci. Technol.* **2017**, *47*, 1763–1782. [[CrossRef](#)]
6. Owens, J. Greenhouse gas emission reductions through use of a sustainable alternative to SF<sub>6</sub>. In Proceedings of the 2016 IEEE Electrical Insulation Conference (EIC), Montreal, QB, Canada, 19–22 June 2016; pp. 535–538.
7. IPCC. *Climate Change 2013: The Physical Science Basis. Contribution of Working Group I to the Fifth Assessment Report of the Intergovernmental Panel on Climate Change*; Stocker, T.F., Qin, D., Plattner, G.-K., Tignor, M., Allen, S.K., Boschung, J., Nauels, A., Xia, Y., Bex, V., Midgley, P.M., Eds.; Cambridge University Press: Cambridge, UK; New York, NY, USA, 2013; p. 1535.
8. Li, Y.; Zhang, X.; Zhang, J.; Fu, M.; Zhuo, R.; Luo, Y.; Chen, D.; Xiao, S. Experimental study on the partial discharge and AC breakdown properties of C<sub>4</sub>F<sub>7</sub>N/CO<sub>2</sub> mixture. *High Volt.* **2019**, *4*, 12–17. [[CrossRef](#)]
9. Rogelj, J.; den Elzen, M.; Höhne, N.; Fransen, T.; Fekete, H.; Winkler, H.; Chaeffer, R.S.; Ha, F.; Riahi, K.; Meinshausen, M. Paris Agreement climate proposals need a boost to keep warming well below 2 °C. *Nature* **2016**, *534*, 631. [[CrossRef](#)] [[PubMed](#)]
10. Li, Y.; Zhang, X.; Chen, D.; Li, Y.; Zhang, J.; Cui, Z.; Xiao, S.; Tang, J. Theoretical study on the interaction between C5-PFK and Al (1 1 1), Ag (1 1 1): A comparative study. *Appl. Surf. Sci.* **2019**, *464*, 586–596. [[CrossRef](#)]
11. Romero, A.; Racz, L.; Matrai, A.; Bokor, T.; Cselko, R. A review of sulfur-hexafluoride reduction by dielectric coatings and alternative gases. In Proceedings of the 2017 6th International Youth Conference on Energy (IYCE), Budapest, Hungary, 21–24 June 2017.
12. Kieffel, Y.; Biquez, F.; Ponchon, P. Alternative gas to SF<sub>6</sub> for use in high voltage switchgears: g3. In Proceedings of the 23rd International Conference on Electricity Distribution, Lyon, France, 15–18 June 2015; p. 0230.
13. De Urquijo, J.; Castrejon-Pita, A.A.; Hernandez-Avila, J.L.; Basurto, E. Electron transport and effective ionization coefficients in C<sub>2</sub>F<sub>6</sub>, C<sub>2</sub>F<sub>6</sub>-Ar and C<sub>2</sub>F<sub>6</sub>-N<sub>2</sub> mixtures. *J. Phys. D Appl. Phys.* **2004**, *37*, 1774. [[CrossRef](#)]
14. Yamamoto, O.; Takuma, T.; Hamada, S.; Yamakawa, Y.; Yashima, M. Applying a gas mixture containing c-C<sub>4</sub>F<sub>8</sub> as an insulation medium. *IEEE Trans. Dielectr. Electr. Insul.* **2001**, *8*, 1075–1081. [[CrossRef](#)]
15. Wada, J.; Ueta, G.; Okabe, S.; Hikita, M. Dielectric properties of gas mixtures with per-fluorocarbon gas and gas with low liquefaction temperature. *IEEE Trans. Dielectr. Electr. Insul.* **2016**, *23*, 838–847. [[CrossRef](#)]
16. Xiao, S.; Zhang, X.; Han, Y.; Dai, Q. AC breakdown characteristics of CF<sub>3</sub>I/N<sub>2</sub> in a non-uniform electric field. *IEEE Trans. Dielectr. Electr. Insul.* **2016**, *23*, 2649–2656. [[CrossRef](#)]
17. Kieffel, Y.; Biquez, F.; Ponchon, P.; Irwin, T. SF<sub>6</sub> alternative development for high voltage Switchgears. In Proceedings of the IEEE Power & Energy Society General Meeting, Denver, CO, USA, 26–30 July 2015.
18. Preve, C.; Piccoz, D.; Maladen, R. Application of HFO1234zeE in MV switchgear AS SF<sub>6</sub> alternative gas. *CIREN-Open Access Proc. J.* **2017**, *2017*, 42–45. [[CrossRef](#)]
19. Li, Y.; Zhang, X.; Zhang, J.; Xiao, S.; Xie, B.J.; Chen, D.C.; Gao, Y.D.; Tang, J. Assessment on the toxicity and application risk of C<sub>4</sub>F<sub>7</sub>N: A new SF<sub>6</sub> alternative gas. *J. Hazard. Mater.* **2019**, *368*, 653–660. [[CrossRef](#)] [[PubMed](#)]
20. Preve, C.; Piccoz, D.; Maladen, R. *Validation Protocol of Potential SF<sub>6</sub> Alternatives*; MATPOST: Lyon, France, 2015.
21. Li, Y.; Zhang, X.; Chen, Q.; Zhang, J.; Li, Y.; Xiao, S.; Tang, J. Influence of oxygen on dielectric and decomposition properties of C<sub>4</sub>F<sub>7</sub>N-N<sub>2</sub>-O<sub>2</sub> mixture. *IEEE Trans. Dielectr. Electr. Insul.* **2019**, *26*, 1279–1286. [[CrossRef](#)]
22. Linteris, G.; Babushok, V.; Sunderland, P.; Takahashi, F.; Katta, V.; Meier, O. Unwanted combustion enhancement by C<sub>6</sub>F<sub>12</sub>O fire suppressant. *Proc. Combust. Inst.* **2013**, *34*, 2683–2690. [[CrossRef](#)]
23. Zhang, X.; Li, Y.; Tian, S.; Xiao, S.; Chen, D.; Tang, J.; Zhuo, R. Decomposition mechanism of the C5-PFK/CO<sub>2</sub> gas mixture as an alternative gas for SF<sub>6</sub>. *Chem. Eng. J.* **2018**, *336*, 38–46. [[CrossRef](#)]

24. Simka, P.; Ranjan, N. Dielectric strength of C<sub>5</sub> Perfluoroketone. In Proceedings of the 19th International Symposium on High Voltage Engineering, Pilsen, Czech Republic, 23–28 August 2015; pp. 23–28.
25. Preve, C.; Maladen, R.; Piccoz, D. Method for validation of new eco-friendly insulating gases for medium voltage equipment. In Proceedings of the 2016 IEEE International Conference on Dielectrics (ICD), Montpellier, France, 3–7 July 2016; pp. 235–240.
26. Tuma, P.E. Fluoroketone C<sub>2</sub>F<sub>5</sub>C(O)CF(CF<sub>3</sub>)<sub>2</sub>, as a Heat Transfer Fluid for Passive and Pumped 2-Phase Applications. In Proceedings of the 2008 Twenty-Fourth Annual IEEE Semiconductor Thermal Measurement and Management Symposium, San Jose, CA, USA, 16–20 March 2008.
27. Li, Y.; Zhang, X.; Tian, S.; Xiao, S.; Li, Y.; Chen, D. Insight into the decomposition mechanism of C<sub>6</sub>F<sub>12</sub>O-CO<sub>2</sub> gas mixture. *Chem. Eng. J.* **2019**, *360*, 929–940. [[CrossRef](#)]
28. Xu, W.; Jiang, Y.; Ren, X. Combustion promotion and extinction of premixed counterflow methane/air flames by C<sub>6</sub>F<sub>12</sub>O fire suppressant. *J. Fire Sci.* **2016**, *34*, 289–304. [[CrossRef](#)]
29. Tian, S.; Zhang, X.; Xiao, S.; Deng, Z.; Li, Y.; Tang, J. Experimental research on insulation properties of C<sub>6</sub>F<sub>12</sub>O/N<sub>2</sub> and C<sub>6</sub>F<sub>12</sub>O/CO<sub>2</sub> gas mixtures. *IET Gener. Transm. Distrib.* **2018**, *13*, 417–422. [[CrossRef](#)]
30. Mantilla, J.; Gariboldi, N.; Grob, S.; Claessens, M. Investigation of the insulation performance of a new gas mixture with extremely low GWP. In Proceedings of the 2014 Electrical Insulation Conference (EIC), Philadelphia, PA, USA, 8–11 June 2014; pp. 469–473.
31. Li, Y.; Zhang, X.; Tian, S.; Xiao, S.; Chen, Q.; Chen, D.; Cui, Z.; Tang, J. Insight into the compatibility between C<sub>6</sub>F<sub>12</sub>O and metal materials: Experiment and theory. *IEEE Access* **2018**, *6*, 58154–58160. [[CrossRef](#)]
32. Tian, S.; Zhang, X.; Xiao, S.; Chen, Q.; Li, Y. Application of C<sub>6</sub>F<sub>12</sub>O/CO<sub>2</sub> mixture in 10 kV medium-voltage switchgear. *IET Sci. Meas. Technol.* **2019**, *13*, 1225–1230. [[CrossRef](#)]
33. Yogeswari, S.; Ramalakshmi, S.; Neelavathy, R.; Johnpaul, M. Identification and comparative studies of different volatile fractions from *Monochaetia kansensis* by GCMS. *Glob. J. Pharmacol.* **2012**, *6*, 65–71.



© 2019 by the authors. Licensee MDPI, Basel, Switzerland. This article is an open access article distributed under the terms and conditions of the Creative Commons Attribution (CC BY) license (<http://creativecommons.org/licenses/by/4.0/>).